Identification of an upstream regulatory pathway controlling actin-mediated apoptosis in yeast

Campbell W. Gourlay and Kathryn R. Ayscough*

Department of Molecular Biology and Biotechnology, Firth Court, University of Sheffield, Western Bank, Sheffield, S10 2TN, UK

*Author for correspondence (e-mail: k.ayscough@sheffield.ac.uk)

Accepted 17 February 2005
Journal of Cell Science 118, 2119-2132 Published by The Company of Biologists 2005
doi:10.1242/jcs.02337

Summary

The build up of reactive oxygen species (ROS) is known to contribute to a reduction in the lifespan of a cell and to their degeneration in diseases such as Alzheimer's and tissue ischaemia. It is therefore important to elucidate pathways that regulate cellular oxidative stress. We have previously shown that actin dynamics can affect the oxidative-stress burden on a yeast cell and thereby its potential lifespan. To elucidate further the connection between actin dynamics and oxidative stress, we sought to identify regulators of this process. The actin regulatory proteins Sla1p and End3p are important in maintaining a rapid turnover of F-actin in cortical patches. We show that cells expressing a mutated form of Sla1p or lacking End3p display markers of apoptosis such as depolarized mitochondrial membranes and elevated levels of reactive oxygen species. Overexpression of the ubiquitin ligase *RSP5* can alleviate the oxidative-stress phenotype observed in cells lacking End3p by targeting Sla1p to the cortex and restoring actin remodelling capability. We also demonstrate that overexpression of *PDE2*, a negative regulator of the Ras/cAMP pathway rescues actin dynamics, reduces oxidative stress sensitivity and restores viability in *Δend3* cells. Our data suggest, for the first time, that a physiological link exists between actin regulation and cAMP signalling that regulates apoptosis in yeast.

Key words: Cell death, cAMP, CAP/SRV2, Mitochondria, ROS

Introduction

The production of reactive oxygen species (ROS) is an inevitable consequence of aerobic metabolism. Under favourable conditions, in healthy cells, ROS generated during respiration are retained by the mitochondria and reduced by protective enzymes such as superoxide dismutase, catalase and glutathione peroxidase. However, a reduction in protective enzyme activity or an event such as mitochondrial membrane depolarisation can result in the accumulation of ROS in the cytoplasm and lead to an oxidative-stress burden on the cell. Oxidative stress has been implicated as a factor in many biological processes, including cell signalling, ageing and apoptosis, as well as in diseases including cancer, neurodegenerative disorders, atherosclerosis and ischaemia (for reviews, see Droge, 2002; Finkel, 2003; Martindale and Holbrook, 2002). Recent studies have highlighted the deleterious effect that excessive ROS production and release can have on cell viability and longevity (for a review, see Martindale and Holbrook, 2002). The damaging effects of cellular materials by ROS are thought to be directly responsible for some of the adverse effects associated with ageing. Genetic evidence linking oxidative stress to lifespan has been obtained in several model organisms. For example, in *Caenorhabditis elegans*, the *daf-2* mutation promotes longevity by increasing *Mn-SOD* expression (Honda and Honda, 1999). In *Drosophila*, the *mth* mutant has an enhanced lifespan and increased resistance to free-radical exposure (Lin et al., 1998). A mutation in the $p66^{shc}$ protein gave rise to mice with an increased lifespan associated with an increased resistance to oxidative stress (Migliaccio et al., 1999). A role for ROS toxicity in yeast ageing is supported by studies in which oxygen radicals are shown to accumulate in yeast cells after the induction of apoptosis (Madeo et al., 1999). A reduction in superoxide-dismutase activity has been shown to reduce cell viability (Longo et al., 1996; Wawryn et al., 1999), and increasing the burden of atmospheric oxygen on yeast cells lacking catalase reduces cell viability (Nestelbacher et al., 2000). In yeast, ageing and apoptosis have been linked (for review, see Jazwinski, 2002). Comparisons of aged mother cells with young virgin cells has revealed that the former exhibit many typical characteristics of apoptosis (Laun et al., 2001).

The discovery that yeast cells display apoptosis-like characteristics has validated yeast as a model system in which to study aspects of programmed cell death in higher eukaryotes (Fröhlich and Madeo, 2001; Can and Reed., 2002; Tissenbaum and Guarente, 2002). Studies that have expressed certain mammalian genes in yeast have suggested that the basic machinery of apoptosis has been evolutionarily conserved. Expression of the mammalian pro-apoptotic gene *Bax* can induce cell death in yeast that is accompanied by typical signs of apoptosis (Ligr et al., 1998). This lethal phenotype can be suppressed by expression of the mammalian anti-apoptotic gene *Bcl-2*, suggesting that yeast has apoptotic pathways. Markers of apoptosis were also associated with yeast cell death after treatment with acetic acid, H_2O_2 and ultraviolet irradiation (Ludovico et al., 2001; Del Carratore et al., 2002).

The actin cytoskeleton is a dynamic structure whose organization by actin-binding proteins (ABPs) facilitates its

Journal of Cell Science

Journal of Cell Science

participation in a diverse array of cellular processes (Ayscough et al., 1997; Drubin et al., 1988; Karpova et al., 1995). There is a close association between actin organization and mitochondrial function. In particular, the actin cytoskeleton has been implicated in the movement of mitochondria along actin filaments via an ARP2/3-dependent propulsion mechanism (Boldogh et al., 2001). Actin-cytoskeleton function is also important for the correct inheritance of mitochondria from the mother cell to the newly forming bud (Simon et al., 1997). A link between the actin-regulatory protein gelsolin and mitochondrially induced apoptosis has also been described in mammalian cells (Ohtsu et al., 1997; Koya et al., 2000). Koya and colleagues demonstrated that overexpression of gelsolin prevented a loss of mitochondrial membrane potential, cytochrome *c* release and subsequent apoptosis in Jurkat cells (Koya et al., 2000).

Recently, we demonstrated that the dynamic state of the actin cytoskeleton is also important for maintaining the membrane potential of mitochondria in yeast (Gourlay et al., 2004). A reduction in actin dynamics caused by mutations in actin itself lead to the development of apoptotic phenotypes such as a loss of mitochondrial membrane potential, elevated ROS levels and DNA fragmentation (Gourlay et al., 2004). Here, we show that the actin-regulatory proteins Sla1p and End3p (Ayscough et al., 1999; Benedetti et al., 1994; Holtzman et al., 1993) and the ubiquitin ligase Rsp5p are upstream regulators of actin-mediated oxidative stress. Loss of Sla1p or Endp3 function results in a less dynamic cytoskeleton, which in turn promotes a loss of mitochondrial membrane potential and an increase in oxidative stress.

We also report that overproduction of the high-affinity cAMP phosphodiesterase PDE2 suppresses the actin defects and associated oxidative-stress phenotype observed in *Δend3* cells. PDE2 is a negative regulator of the Ras/cAMP signalling pathway, which links stress response and cell growth to nutrient availability (for a review, see Rolland et al., 2002). Our data provide the first evidence in a eukaryotic system of a physiologically relevant pathway linking nutritional sensing via the Ras/cAMP pathway to actin-mediated apoptosis.

Materials and Methods

Yeast strains, plasmids, media and growth conditions

Yeast strains and plasmids used in this study are listed in Table 1. Unless stated otherwise, cells were grown in a rotary shaker at 30°C in liquid YPD medium (1% yeast extract, 2% Bacto-peptone, 2% glucose, 40 μg ml^{-1} adenine). For glycerol plates, the 2% glucose was replaced with 3% glycerol before pouring plates. *Δend3* strains (KAY450 and KAY451) have the *END3* gene deleted and, for all experiments, were compared with their wild-type parental strain KAY446. The strain *sla1Δ118-511* (KAY350) encodes a truncated form of Sla1p that lacks residues 118-511 and was compared with its parental wild type KAY36. KAY116 is the parental strain that was used to integrate the *end3-1* allele (KAY117). KAY116 and KAY117 were directly compared in the experiments carried out in this study. The rho^0 strains of KAY350 and KAY450 were generated by ethidium-bromide treatment as described (Guthrie and Fink, 1991). The plasmids for overexpression of *RSP5* (YCpHA-RSP5) and control (YCp) have previously been described (Kaminska et al., 2002).

Multicopy suppressor screen

1×10^5 *Δend3* cells (KAY450) were transformed with 20 μg genomic library constructed in YEp13 [a kind gift from P. Sudbery, originally purchased from the ATCC (http://www.atcc.org/)], plated onto YPD medium containing 1.5 mM H_2O_2 and incubated at 30°C for 3 days. KAY450 cells exhibit restricted growth under these conditions. Surviving colonies were sequentially replica plated onto YPD medium containing 2 mM H_2O_2, 2.5 mM H_2O_2 and then 3 mM H_2O_2. 16 colonies were isolated on 3 mM H_2O_2, the plasmids rescued and retransformed into KAY450 cells. All rescued plasmids retransformed into KAY450 cells allowed growth on medium containing 3 mM H_2O_2.

Reactive oxygen species detection using flow cytometry

Cells were incubated overnight in the presence of 5 μg ml^{-1} 2′,7′-dichlorodihydrofluorescein diacetate (H_2DCFDA; Molecular Probes). Cells were sonicated before analysis; fluorescence was then analysed using a Becton-Dickinson Flow Cytometer. Fluorescence-activated cell sorting (FACS) parameters were set at excitation and emission settings of 304 nm and 551 nm (filter FL-1), respectively.

Viability assays

Assays were carried out as previously described (Gourlay et al., 2004). Briefly, cells were grown in liquid YPD medium. Cell number was determined in triplicate, with a Schärfe Systems TT Cell Counter and Analyser. Serial dilutions were plated onto YPD agar plates and the number of surviving colonies was counted. The viability was determined by dividing the number of surviving colonies by the calculated number of plated colonies and multiplying by 100 to give a percentage.

Fluorescence microscopy

Rhodamine-phalloidin and DAPI staining was performed as previously described for F-actin (Hagan and Ayscough, 2000). Cells were processed for immunofluorescence microscopy as described previously (Ayscough and Drubin, 1998). Antibodies were used to detect Srv2p (a gift from D. Drubin, University of California at Berkeley, CA) by immunofluorescence microscopy at 1:50 dilution. Secondary antibodies used were fluorescein isothiocyanate (FITC) conjugated goat anti-rabbit antibodies (Vector Laboratories) at 1:100 dilution. Cells were viewed with an Olympus BX-60 fluorescence microscope with a 100 W mercury lamp and an Olympus 100× Plan-

Table 1. Yeast strains and plasmids used in this study

Strain	Relevant genotype	Origin
KAY446	*Mata his3Δ1 leu2Δ met15Δ ura3Δ*	Research genetics
KAY450	*Mata Δend3::KanMx his3Δ1 leu2Δ met15Δ ura3Δ*	Research genetics
KAY451	*Matα Δend3::KanMx his3Δ1 leu2Δ lys2Δ ura3Δ*	Research genetics
KAY36	*Mata his3-Δ200 leu2-3,112 ura3-52, lys2-801^{am}*	D. Drubin (University of California at Berkeley) (†DDY903)
KAY350	*Mata his3-Δ200 leu2-3,112 ura3-52, lys2-801^{am} sla1ΔR1::HIS3 sla1-Δ2::LEU2*	Gourlay et al., 2003
KAY116	*Mata ura3 leu2 his4 bar1-1*	H. Riezman (Basel, Switzerland) (†RH144-5D)
KAY117	*Mata end3-1 ura3 leu2 his4 bar1-1*	H. Riezman (Basel, Switzerland) (†RH266-1D)

†Original strain accession numbers.

Journal of Cell Science

NeoFluar oil-immersion objective. Images were captured using a Roper Scientific Micromax 1401E cooled CCD camera using IP lab software (Scanalytics, Fairfax, VA) on an Apple Macintosh G4 computer.

Hydrogen-peroxide- and latrunculin-A-sensitivity halo assays

10 µl overnight culture was added to 2 ml YPD and 2 ml 1% sterile agar. The cells were poured onto a YPAD plate and cooled, and then sterile disks containing 10 µl hydrogen peroxide at concentrations of 1%, 2%, 3% and 5%, or latrunculin-A (LatA) at 2 mM and 5 mM were placed onto each plate. Each plate was performed in triplicate for each strain. Plates were incubated at 30°C for 3 days and then halo radii were measured in mm. To obtain the relative sensitivity to hydrogen peroxide, the logarithm of the hydrogen-peroxide concentration ($\log[H_2O_2]$) was plotted as a function of halo diameter in mm, curve fits were obtained and the $[H_2O_2]$ required to give a halo diameter of 21 mm was calculated. These amounts were then normalized to that of the wild type and their inverse was taken to determine the relative apparent sensitivity of each strain to H_2O_2.

Mitochondrial visualization and inhibition

Mitochondria were visualized using using either 3,3′-dihexyloxacarbocyanine iodide [$DiOC_6(3)$] at 20 ng/ml as previously described (Simon et al., 1997) or a mitochondrion-targeted green fluorescent protein (GFP) as described previously (Westermann and Neupert, 2000). The mitochondrial inhibitor antimycin A (Sigma) was added to liquid cultures at a concentration of 0.1 mg ml^{-1}. This concentration was sufficient to inhibit the build up of detectable ROS in overnight cultures but did not affect cell number when a assayed using a Schärfe Systems TT Cell Counter and Analyser.

Phosphatidylserine exposure

Phosphatidylserine (PS) exposure was assayed using FITC/annexin-V as previously described (Madeo et al., 1997). Briefly, 1×10^6 cells were washed twice in 200 µl digestion buffer (1.2 M sorbitol, 0.5 mM $MgCl_2$, 35 mM K_2HPO_4, pH 6.8) and resuspend in 15 U ml^{-1} lyticase, 2% glusulase. Cells were incubated at 30°C for 2 hours and washed twice in 200 µl annexin-V binding buffer (Roche) containing 1.2 M sorbitol. Cells were then resuspend in 39 µl annexin-V binding buffer containing 1 µl FITC/annexin-V (Roche) and incubated at room temperature for 30 minutes. Cells were washed twice in binding buffer and analysed by flow cytometry. Using a Becton-Dickinson Flow Cytometer. FACS parameters were set at excitation and emission settings of 304 nm and 551 nm (filter FL-1), respectively.

Caspase activity

In vivo staining of caspase activity by flow cytometry was carried out using a staining solution containing FITC–VAD-fmk (CaspACE™, Promega) as previously described (Madeo et al., 2002a).

Glycogen staining and heat-shock sensitivity

Iodine staining of yeast cells as an assay for glycogen content was carried out as previously described (Care et al., 2004). Heat-shock sensitivity was carried out as previously described (Sass et al., 1986).

Results

Identification of proteins involved in coupling actin dynamics to oxidative stress

Our previous studies demonstrated that a reduction in F-actin dynamics caused by mutations in the actin-encoding gene leads to elevated ROS production from the mitochondria and a consequent loss of viability (Gourlay et al., 2004). We postulated that one physiological role of such a pathway in yeast would be to regulate appropriate responses to environmental stresses. These environmental cues would then function through regulation of proteins that control actin dynamics. An inability to grow on the non-fermentable carbon source glycerol correlated with reduced actin dynamics and ROS accumulation (Gourlay et al., 2004). We therefore screened several strains deleted for actin-regulatory genes for their ability to grow on glycerol-containing medium. Strains deleted for *SLA1*, *END3*, *SLA2*, *ARK1*, *PRK1*, *ABP1*, *RVS167*, *SCP1*, *TPM1*, *LAS17*, *SAC6* and *YSC84*, and lacking the actin-regulatory region of *SLA1* (*sla1Δ118-511*) were tested. We consistently found that *Δend3* and *sla1Δ118-511* cells were unable to use glycerol as a carbon source, indicating that these mutants possessed

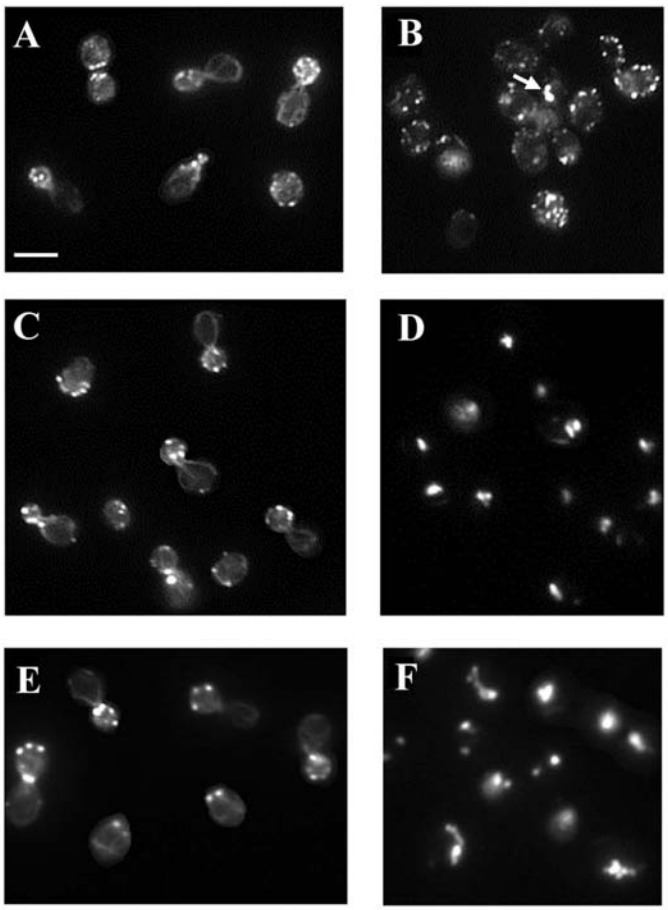

Fig. 1. F-Actin is less dynamic in *Δend3* and *sla1Δ118-511* cells. F-Actin in cells from low- and high-density cultures (log and early stationary phase) was visualized by fluorescent microscopy using rhodamine-phalloidin. In wild-type cells during log phase, actin patches polarize to areas of new cell growth (A) but, in *Δend3* (C) and *sla1Δ118-511* (E) cells, cortical patches (while still polarized) were larger and less numerous. During early stationary phase, actin patches become depolarized and numerous in wild-type cells (B), and large F-actin aggregates were observed in a small proportion (<5%) of cells (arrowhead). By contrast, *Δend3* (D) and *sla1Δ118-511* (F) F-actin appears as large aggregates in most (>95%) cells. Bar, 10 µm.

Journal of Cell Science

respiratory defects. Therefore, *Δend3* and *sla1Δ118-511* strains were selected for further analysis.

Δend3 and *sla1Δ118-511* cells accumulate F-actin aggregates

Wild-type budding yeast cells display a distinct alteration in cortical actin distribution between logarithmic- and stationary-phase growth. In the logarithmic phase of growth, wild-type cells possess a polarized actin phenotype with cortical patches concentrated at areas of cell growth (Fig. 1A). In stationary-phase culture, the cytoskeleton becomes depolarized and actin patches can be visualized throughout the cell (Fig. 1B). In a small proportion of wild-type stationary-phase cells, F-actin appears in large aggregates (Fig. 1B, arrowhead). In *Δend3* and *sla1Δ118-511* cells in log phase, cortical actin patches are also polarized but appear to be fewer in number and are larger (or 'chunkier') in appearance (Fig. 1C,E). Strikingly, during the stationary phase, the F-actin within cells exists as large aggregates (Fig. 1D,F). Cells deleted for *SLA1* show a less severe actin-clumping phenotype (data not shown), suggesting that the *sla1Δ118-511* mutation causes a dominant-negative phenotype. Both *Δend3* and *sla1Δ118-511* cells are resistant to the actin-depolymerizing drug LatA, suggesting that both display reduced actin dynamics (data not shown).

Δend3 and *sla1Δ118-511* cells display respiratory defects

Cells lacking *end3* or expressing *sla1Δ118-511* were also not able to grow on the non-fermentable carbon source glycerol (Fig. 2A). The inability to use glycerol suggests that *Δend3* and

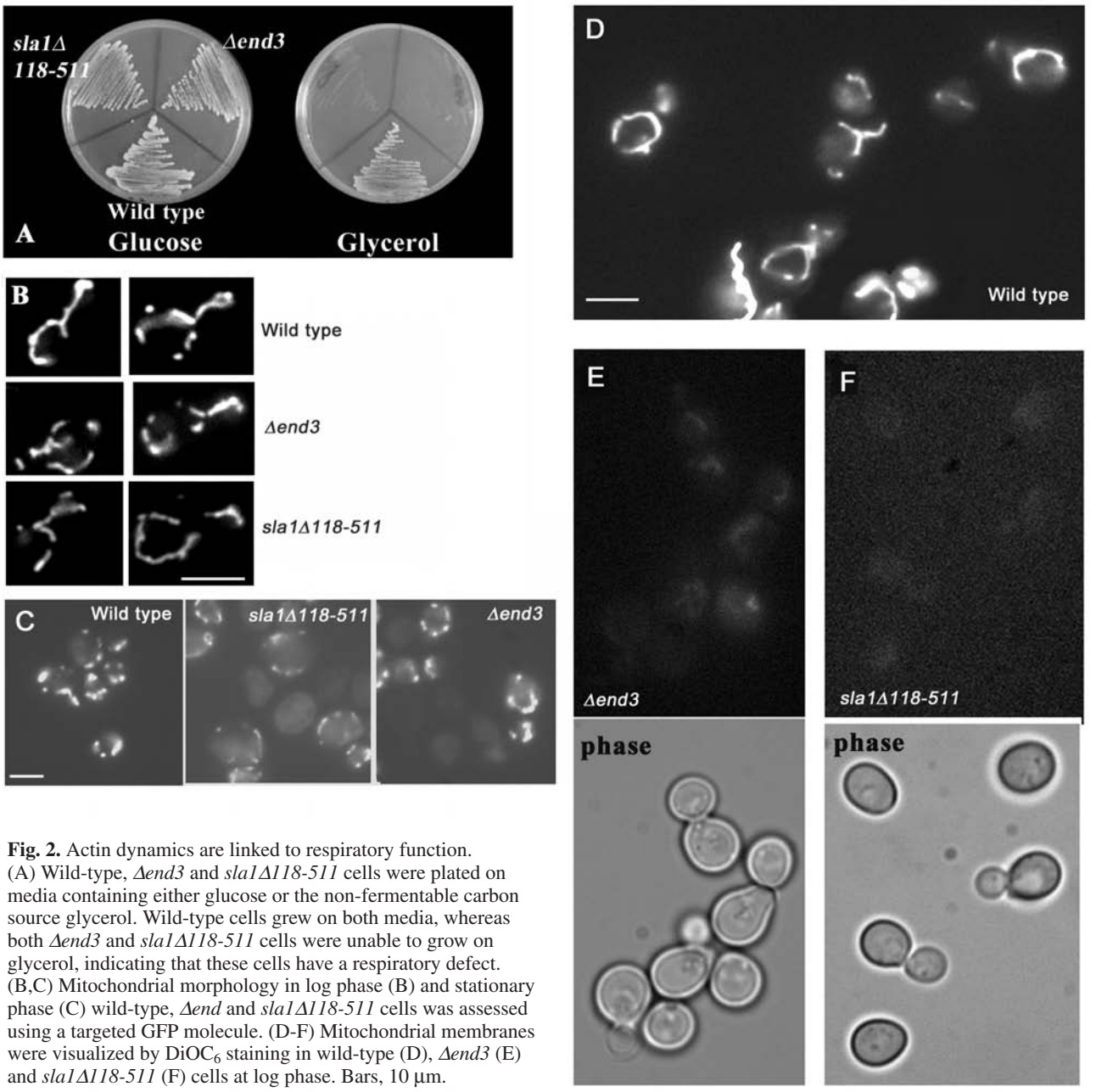

Fig. 2. Actin dynamics are linked to respiratory function. (A) Wild-type, *Δend3* and *sla1Δ118-511* cells were plated on media containing either glucose or the non-fermentable carbon source glycerol. Wild-type cells grew on both media, whereas both *Δend3* and *sla1Δ118-511* cells were unable to grow on glycerol, indicating that these cells have a respiratory defect. (B,C) Mitochondrial morphology in log phase (B) and stationary phase (C) wild-type, *Δend* and *sla1Δ118-511* cells was assessed using a targeted GFP molecule. (D-F) Mitochondrial membranes were visualized by $DiOC_6$ staining in wild-type (D), *Δend3* (E) and *sla1Δ118-511* (F) cells at log phase. Bars, 10 μm.

Journal of Cell Science

sla1Δ118-511 cells have a respiratory defect. The actin cytoskeleton has been demonstrated to be important in the regulation of mitochondrial movement, morphology and inheritance in budding yeast. To investigate whether the actin-regulating proteins Sla1p and End3p play roles in mitochondrial regulation, we examined mitochondrial morphology, DNA presence and membrane potential. Cells expressing mitochondrion-targeted GFP were visualized by fluorescence microscopy. Cells in the log phase of growth showed a similar morphology in both wild-type and mutant cells (Fig. 2B). Mitochondrial membranes appeared as either punctate or tubular formations that were distributed in both the mother and the bud (Fig. 2B). No significant defect in inheritance was observed in mutant cells – mitochondrial membranes appeared to be transported into the buds of mutant cells as in the wild type. It should be realized that levels of the mitochondrial membrane protein porin were identical in wild-type and mutant log-phase cells when assayed by western blotting (data not shown). In the stationary phase, cells' mitochondrial membranes appeared punctate in wild-type, *slaΔ118-511* and *Δend3* cells (Fig. 2C). However, a large proportion of cells in *slaΔ118-511* and *Δend3* cultures displayed diffuse staining with no obvious mitochondrial membrane staining (Fig. 2C). $DiOC_6$ was used to visualize mitochondrial membranes in wild-type, *sla1Δ118-511* and *Δend3* cells during log phase (Fig. 2D-F). At a concentration of 20 ng ml^{-1}, this dye accumulates specifically at mitochondrial membranes and can be observed by fluorescence microscopy. However, cells that have low mitochondrial membrane potential will fail to accumulate $DiOC_6$. After $DiOC_6$ staining, wild-type cells showed a similar phenotype to that observed using the targeted GFP (Fig. 2D). However, in both *sla1Δ118-511* and *Δend3* cells, $DiOC_6$ staining was greatly reduced in all cells compared with the wild type (Fig. 2E,F). The same result was observed in cells grown to stationary phase (data not shown). This demonstrates a reduction in mitochondrial membrane potential in *sla1Δ118-511* and *Δend3* cells throughout growth in culture. It should also be realized that during log-phase growth, mitochondrial DNA was present in wild-type and mutant cells, as observed by DAPI staining (data not shown). These data demonstrate that the respiratory defect, highlighted by the glycerol growth defect observed in *sla1Δ118-511* and *Δend3* cells, correlates with a reduction in mitochondrial membrane potential rather than gross morphological or inheritance defects.

Δend3 and *sla1Δ118-511*cells show elevated ROS levels and H_2O_2 sensitivity

A reduction in mitochondrial membrane potential is often associated with an increase in cytoplasmic ROS accumulation. To investigate this, *Δend3* and *sla1Δ118-511* cells were grown in the presence of the indicator dye H_2DCFDA and assessed by flow cytometry. Wild-type cells grown overnight to early stationary phase typically displayed two peaks of fluorescence representing populations with low (M1) and high (M2) ROS levels (Fig. 3A). Most wild-type cells were contained in the M1 population. In *Δend3* and *sla1Δ118-511* cells, a dramatic shift was observed to a high-ROS-accumulating M2 population. Quantification of this event revealed that the average proportion of wild-type cells in M2 was 21±2% (Fig. 3B). In *Δend3* and *sla1Δ118-511* cells, the M2 population was 83±4% and 97±1%, respectively (Fig. 3B). In agreement with this increase in ROS accumulation, *Δend3* and *sla1Δ118-511* cells both displayed an increased sensitivity to H_2O_2 (Fig. 3C). Using a halo assay approach, it was calculated that *Δend3* and *sla1Δ118-511* mutants had 1.7 and 2.0 times greater sensitivity than wild-type cells, respectively (Fig. 3C).

In order to establish the origin of the ROS that accumulate in *Δend3* and *sla1Δ118-511* cells, we generated rho^0 yeast strains (which lack mitochondrial DNA) by ethidium-bromide treatment (Fig. 3D). The ROS accumulation observed in *Δend3* and *sla1Δ118-511* cells (Fig. 3A) was not observed in the rho^0 strains. This confirms that ROS accumulation is of mitochondrial origin. To address whether the ROS are a byproduct of the mitochondrial electron-transport chain, we made use of the complex-III inhibitor antimycin A. A concentration of 0.1 mg ml^{-1} in liquid cultures was found to have no effect on growth of *Δend3* or *sla1Δ118-511* cells (data not shown) but was sufficient to inhibit the build up of detectable ROS (Fig. 3D). No significant difference was observed in F-actin distribution between rho^+ and rho^0 cells (data not shown), demonstrating that ROS accumulation lies downstream of the actin-cytoskeleton phenotype.

A loss of mitochondrial membrane potential and an increase in ROS have been linked to the onset of apoptosis. An early marker for the apoptotic process is the exposure of phosphatidylserine on the surface of cells (Madeo et al., 1997). Phosphatidylserine can be assayed in yeast cells that have had their cell walls disrupted using a FITC-labelled annexin-V substrate. The addition of sublethal amounts of H_2O_2 to cultures grown to log phase was used to assay the effects on phosphatidylserine exposure using FITC/annexin-V (Fig. 3E). This experiment was carried out in triplicate and a representative data set is presented. Although no PS exposure was detected in wild-type cells over a 0.0-0.6 mM range, both *Δend3* and *sla1Δ118-511* showed a dose-dependent increase in the number of cells displaying a high fluorescence, suggesting that a greater proportion of the population was entering apoptosis. This data suggests that *Δend3* and *sla1Δ118-511* cells undergo apoptosis in response to low levels of H_2O_2, in agreement with their relative sensitivity as observed by the halo assay approach (Fig. 3C).

Reduction in actin dynamics leads to apoptosis in *end3-1* cells

As yeast cells exit the log phase of growth, they have to change their metabolic strategy from a primarily fermentative one to aerobic respiration. This metabolic change is referred to as the diauxic shift. In the experiments described above, the accumulation of ROS in *Δend3* and *sla1Δ118-511* cells was assessed in cultures grown overnight to stationary phase. Therefore, the increase in mitochondrial activity upon entry into stationary phase, coupled with reduced mitochondrial membrane potential, might give rise to ROS accumulation. To assess whether a reduction in actin dynamics can lead to apoptosis in cells in the log phase of growth, we analysed cells expressing the temperature-sensitive *end3-1* allele (Benedetti et al., 1994). At 24°C, *end3-1* cells display a wild-type actin-cytoskeleton phenotype at log phase, with punctate actin patches polarized to sites of cell growth (Fig. 4A) (Warren et

Journal of Cell Science

al., 2002). When shifted to 37°C for 2 hours, the actin cytoskeleton closely resembles that of *Δend3* cells. Cortical actin structures become fewer and larger, suggesting a slowing down of cytoskeletal dynamics (Fig. 4A) (Warren et al., 2002). To test for a respiratory defect, *end3-1* mutant cells were plated on media containing either glucose or glycerol as the sole carbon source at 24°C or 37°C (Fig. 4B). Cells expressing the *end3-1* allele grew at 24°C and 37°C on glucose-containing medium but only at 24°C on glycerol-containing plates. The inability of *end3-1* cells to grow at 37°C on glycerol-containing medium suggests a temperature-sensitive respiratory defect. Wild-type, *Δend3* and *sla1Δ118-511* cells were also tested and all grew at both temperatures on glucose plates. As expected, *Δend3* and *sla1Δ118-511* cells could not grow at either temperature on glycerol-containing medium (Fig. 4B).

In order to examine the nature of the temperature-sensitive respiratory defect, wild-type and *end3-1* mutant cells were grown to log phase at 24°C before being shifted to 37°C for 2 hours. We used a mitochondrion-targeted GFP to examine morphological changes in response to the temperature shift. In wild-type cells, temperature shift had a small effect on mitochondrial morphology, with cells showing a more punctate appearance than observed at 24°C (Fig. 4C). *end3-1* cells incubated at 37°C for 2 hours displayed a similar increase in mitochondrial membrane disorganization to those incubated at 24°C. At 24°C, mitochondrial membranes were clearly visible in log-phase cells when stained with $DiOC_6$ (Fig. 4D). Strikingly, after 2 hours at 37°C, *end3-1* cells displayed a severe reduction in mitochondrial membrane staining, demonstrating a rapid reduction in mitochondrial membrane potential (Fig. 4D).

At 24°C, both log-phase wild-type and log-phase *end3-1* cells showed low levels of ROS accumulation, with most of the population appearing in the M1 peak (Fig. 5A). No significant accumulation of ROS was detected in wild-type cells when shifted to 37°C for 2 hours (Fig. 5A). However under the same conditions, a significant accumulation of ROS was observed in *end3-1* cells (Fig. 5A).

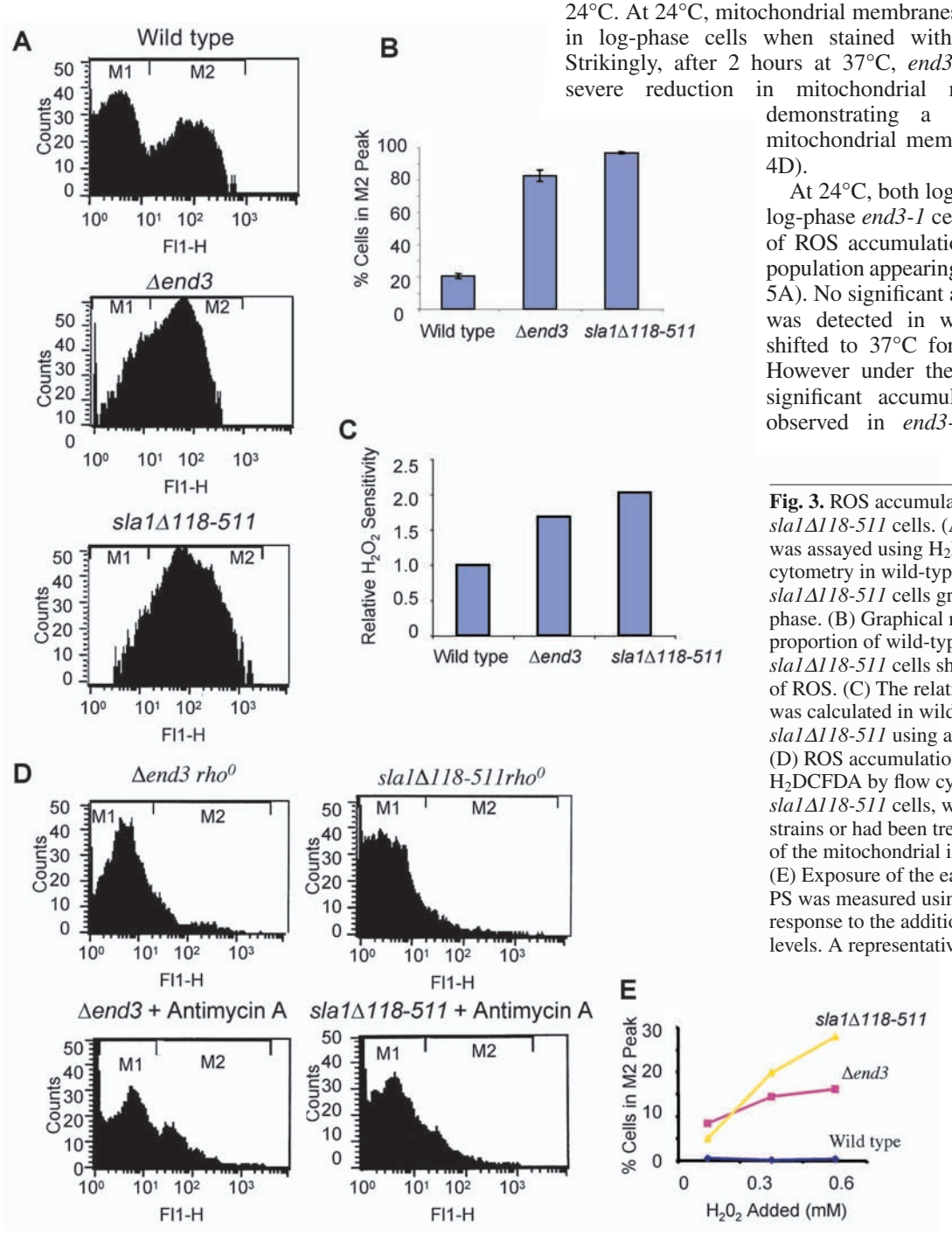

Fig. 3. ROS accumulation in *Δend3* and *sla1Δ118-511* cells. (A) ROS accumulation was assayed using H_2DCFDA by flow cytometry in wild-type, *Δend3* and *sla1Δ118-511* cells grown to early stationary phase. (B) Graphical representation of the proportion of wild-type, *Δend3* and *sla1Δ118-511* cells showing a high build up of ROS. (C) The relative sensitivity to H_2O_2 was calculated in wild-type, *Δend3* and *sla1Δ118-511* using a halo-assay approach. (D) ROS accumulation was assessed using H_2DCFDA by flow cytometry in *Δend3* and *sla1Δ118-511* cells, which were either *rho*^{0} strains or had been treated with 0.1 mg ml^{-1} of the mitochondrial inhibitor antimycin A. (E) Exposure of the early apoptotic marker PS was measured using FITC/annexin-V in response to the addition of H_2O_2 at sublethal levels. A representative data set is shown.

Interestingly the loss of mitochondrial membrane potential and ROS accumulation in *end3-1* cells at the restrictive temperature was also accompanied by significant activation of yeast caspase, as assayed using FITC–VAD-fmk (Fig. 5B) (Madeo et al., 2002a). Wild-type cells showed no increase in caspase activation when shifted to 37°C for 2 hours (Fig. 5B). To demonstrate the physiological significance of mitochondrial membrane potential loss, ROS accumulation and caspase activation, wild-type and *end3-1* cells were assayed for viability using the same temperature shift and culture conditions (Fig. 5C). Wild-type cells showed no significant loss in viability on temperature shift. By contrast, although *end3-1* viability was similar to that of the wild type at 24°C, it fell dramatically after incubation at 37°C for 2 hours (Fig. 5C). These data support a pathway that leads from a reduction of actin dynamics to the development of apoptotic markers and cell death.

Expression of *RSP5* can reduce the oxidative-stress burden of *Δend3* cells, improve their viability and restore actin-remodelling capability

A recent study demonstrated that Sla1p can bind to Rvs167p, suggesting homology to the CIN85-endophilin complex found in mammalian cells (Stamenova et al., 2004). In support of this model is the fact that both yeast and mammalian complexes are regulated by the homologous E3 ubiquitin ligases Rsp5p and NEDD4. Furthermore, the overexpression of *RSP5* has been shown to rescue a growth phenotype seen in *Δend3* cells on glycerol-containing medium (Kaminska et al., 2002). To investigate this further, we overexpressed *RPS5* in *Δend3* cells and analysed the effects on mitochondrial function, ROS generation and viability. In agreement with Kaminska and colleagues (Kaminska et al., 2002), haploid cells lacking *end3* were able to grow at comparable rates to wild type on plates containing glucose but unable to grow on glycerol-containing medium. At 37°C, *Δend3* cells were grew well on glucose-containing plates but were nonviable on glycerol-containing medium (Fig. 6A). Overexpression of *RSP5* in *Δend3* cells was able to restore growth on glycerol-containing plates at 37°C (Fig. 6A). As described earlier, a large ROS accumulation was observed in *Δend3* cells compared with the wild type (Fig. 6B). In accordance with a rescue of respiratory function, the accumulation of ROS in *Δend3* cells was decreased when *RSP5* was overexpressed (Fig. 6B). Because ROS accumulation has an adverse effect on cell viability, we assayed the effect of ROS reduction in *Δend3* cells overexpressing *RSP5*. Cells were

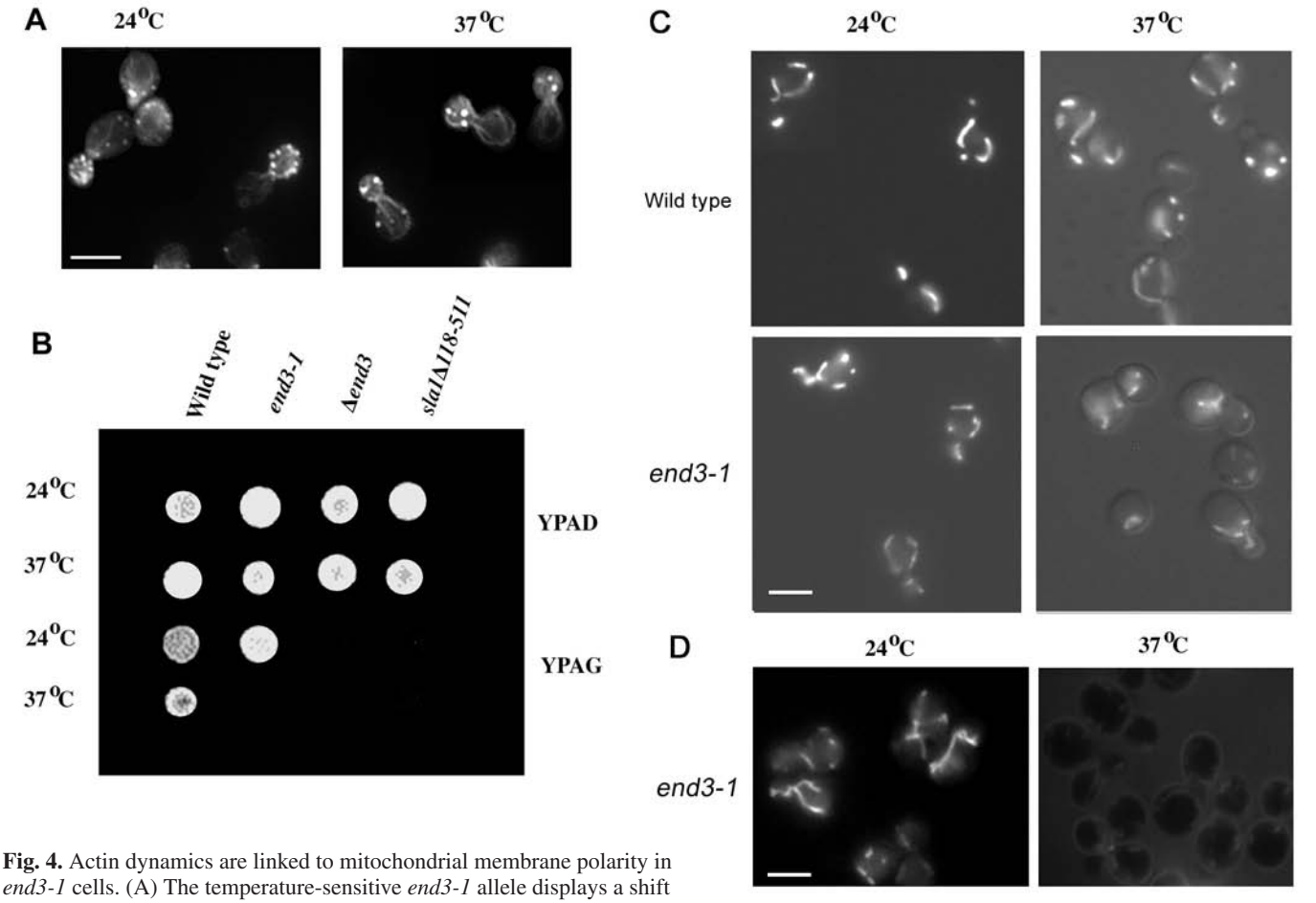

Fig. 4. Actin dynamics are linked to mitochondrial membrane polarity in *end3-1* cells. (A) The temperature-sensitive *end3-1* allele displays a shift from the wild type to the *Δend3* actin phenotype when shifted from 24°C to 37°C for 2 hours. (B) Cells expressing the *end3-1* allele were plated on glucose- or glycerol-containing media at 24°C or 37°C; as positive and negative controls, wild-type, *Δend3* and *sla1Δ118-511* cells were also plated. (C) Mitochondrial morphology was examined using targeted GFP in wild-type and *end3-1* cells at 24°C and after 2 hours of growth at 37°C. (D) Mitochondria were visualized using $DiOC_6$ in *end3-1* cells shifted from 24°C or 37°C for 2 hours. Bar, 10 μm.

grown overnight and the viability of wild-type cells, *Δend3* cells and *Δend3* cells overexpressing *RSP5* was quantified. The results demonstrate a significant increase in viability as a result of *RSP5* overexpression (Fig. 6C). The partial rescue of viability in *Δend3* cells overexpressing *RSP5* agrees with the reduced level of ROS accumulation in these cells. We wished to assess whether the overexpression of *RSP5* in *Δend3* cells could also rescue defects in cytoskeleton organization. F-Actin was visualized in wild-type, *Δend3* and *Δend3[RSP5]* cultures grown to stationary phase. As expected for wild-type cells entering stationary phase, most were round and unbudded. In those cells that were still budding, actin patches occurred throughout the cell. In *Δend3* cells, F-actin patches were fewer and in larger clumps, as has previously been observed (Fig. 6D) (Benedetti et al., 1994; Care et al., 2004). Also as previously reported, a high proportion of cells were budding and had polarized cortical actin patches, suggesting a failure to enter stationary phase. In accordance with this, these cells failed to accumulate glycogen (Fig. 6E). By contrast, *Δend3* cells overexpressing *RSP5* displayed an F-actin staining that was similar to the wild type and cells were predominantly round and unbudded (Fig. 6D), and accumulated glycogen (Fig. 6E). This suggests that the overexpression of *RSP5* increases the ability of *Δend3* cells to enter stationary phase and improves the organization of the F-actin cytoskeleton.

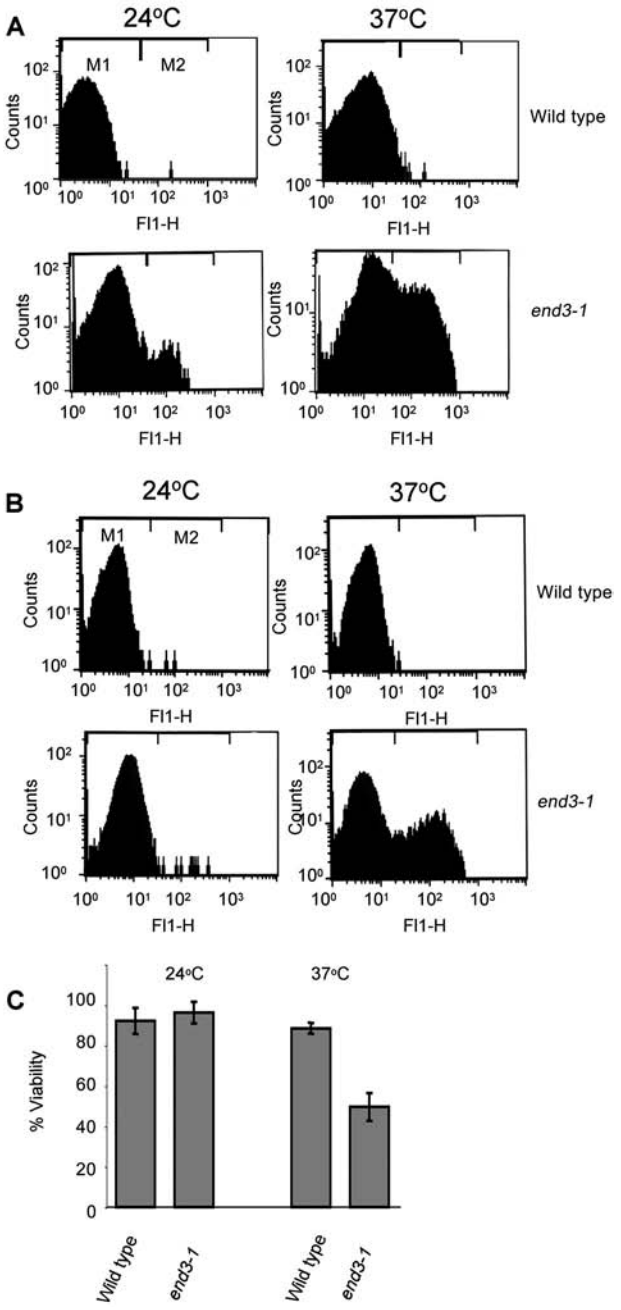

Fig. 5. Actin-stabilized *end3-1* cells display markers of apoptosis. ROS accumulation using H_2DCFDA (A) and caspase activation using FITC–VAD-fmk (B) were measured by flow cytometry in wild-type and *end3-1* cells grown to log phase at 24°C and after 2 hours of growth at 37°C. (C) The viabilities were calculated of wild-type and *end3-1* cultures grown to log phase at 24°C and after a shift to 37°C for 2 hours.

Rsp5p-dependent targeting of Sla1p to the cell cortex

Because *RSP5* overexpression led to the rescue of many of the phenotypes associated with the deletion of *END3*, we considered that high levels of ubiquitination might allow some functions of End3p to be bypassed. One previously identified role of End3p is the targeting of Sla1p to cortical-containing structures (Warren et al., 2002). Fewer punctate Sla1p-GFP spots were observed in *Δend3* cells than in wild type cells and there is a significant level of cytoplasmic staining (Fig. 7A,B) (Warren et al., 2002). As sown in Fig. 7C, overexpression of *RSP5* in *Δend3* cells can restore Sla1p localization to cortical patches and reduce its presence in the cytosol compared with the wild type, and there is a significant reduction in the level of cytoplasmic staining (Fig. 7A,B) (Warren et al., 2002). This suggests a role for Rsp5p in targeting Sla1p to the membrane.

PDE2 overexpression rescues the oxidative-stress phenotype of *Δend3* cells and restores viability

In order to identify upstream regulators of actin-mediated oxidative stress, we carried out a multicopy suppressor screen to identify suppressors of the H_2O_2 sensitivity observed in *Δend3* cells. Of the 16 plasmids that were isolated, eight contained multiple open reading frames and await further analysis. The other eight contained a single open reading frame encoding Pde2p, the yeast high-affinity cAMP phosphodiesterase (Sass et al., 1986), and upstream sequence. *PDE2* is a negative regulator of the Ras/cAMP signalling cascade and an important component of stress management and cell growth in response to nutrient depletion (Sass et al., 1986). The effect of *PDE2* overexpression on H_2O_2 sensitivity in wild-type and *Δend3* cells is shown in Fig. 8A. In order to establish whether the increased H_2O_2 tolerance observed in *Δend3* cells overexpressing *PDE2* correlated with a reduction in ROS accumulation, wild-type and *Δend3* cells containing an empty YEp13 vector or YEp13 containing *PDE2* were grown to early stationary phase, stained with H_2DCFDA and visualized by fluorescence microscopy (Fig. 8B). Cells lacking *end3* displayed a marked increase in ROS accumulation compared with the wild type, as indicated by the elevated levels of fluorescence. Strikingly, the overexpression of *PDE2* resulted

in a substantial reduction in ROS levels in *Δend3* cells (Fig. 8B). We tested whether *PDE2* overexpression led to an improvement in the survival of early-stationary-phase cultures and found that *Δend3* cells possessed a large proportion of nonviable cells compared with the wild type (Fig. 8C). Interestingly, the overexpression of *PDE2* and the concomitant reduction in oxidative stress in *Δend3* cells correlated with a restoration of viability to wild-type levels. A small but significant increase in culture viability was also observed in wild-type cells overexpressing *PDE2* (Fig. 8C).

Actin dynamics are linked to oxidative stress via a Pde2p-dependent mechanism

One hypothesis for our data and that of others is that the Ras/cAMP pathway links environmental stress to F-actin reorganization (Ho and Bretscher, 2001; Hubberstey and Mottillo, 2002). We therefore tested whether the overexpression of *PDE2* in *Δend3* cells in early stationary phase had an effect on F-actin organization. At this stage of growth, all *Δend3* cells displayed aggregated F-actin (Fig. 9A). Overexpression of *PDE2* in these cells resulted in a significant reduction in the formation of F-actin aggregates. To examine whether the reduction in F-actin aggregation correlated with a restoration of cytoskeletal dynamics, we examined the sensitivity of these strains to the actin-monomer-sequestering drug LatA. Cells lacking End3p displayed an increased resistance to LatA, indicating a reduction in actin dynamics (Fig. 9B). *PDE2* overexpression restored LatA sensitivity to *Δend3* cells, indicating an increase in cytoskeletal dynamics. It has previously been demonstrated that the action of Pde2p to lower cAMP levels has an inhibitory effect on cAMP-dependent protein kinase A (PKA) activity. Inhibition of PKA activity has been shown to lead to the accumulation of storage carbohydrates such as glycogen and an increased resistance to heat shock. We wished to examine whether the rescue of oxidative stress by Pde2p in *Δend3* cells was a result of PKA downregulation. Cells lacking *end3* fail to accumulate glycogen (Care et al., 2004) (Fig. 9C), this phenotype is surprisingly not restored by *PDE2* overexpression. Similarly, the heat-shock sensitivity exhibited by *Δend3* cells was not rescued by *PDE2* expression (Fig. 9D). As expected, *PDE2* overexpression in wild-type cells conferred a greater resistance to heat shock. These data suggest that the restoration of actin dynamics and rescue of oxidative stress by *PDE2* is achieved by a PKA-independent pathway.

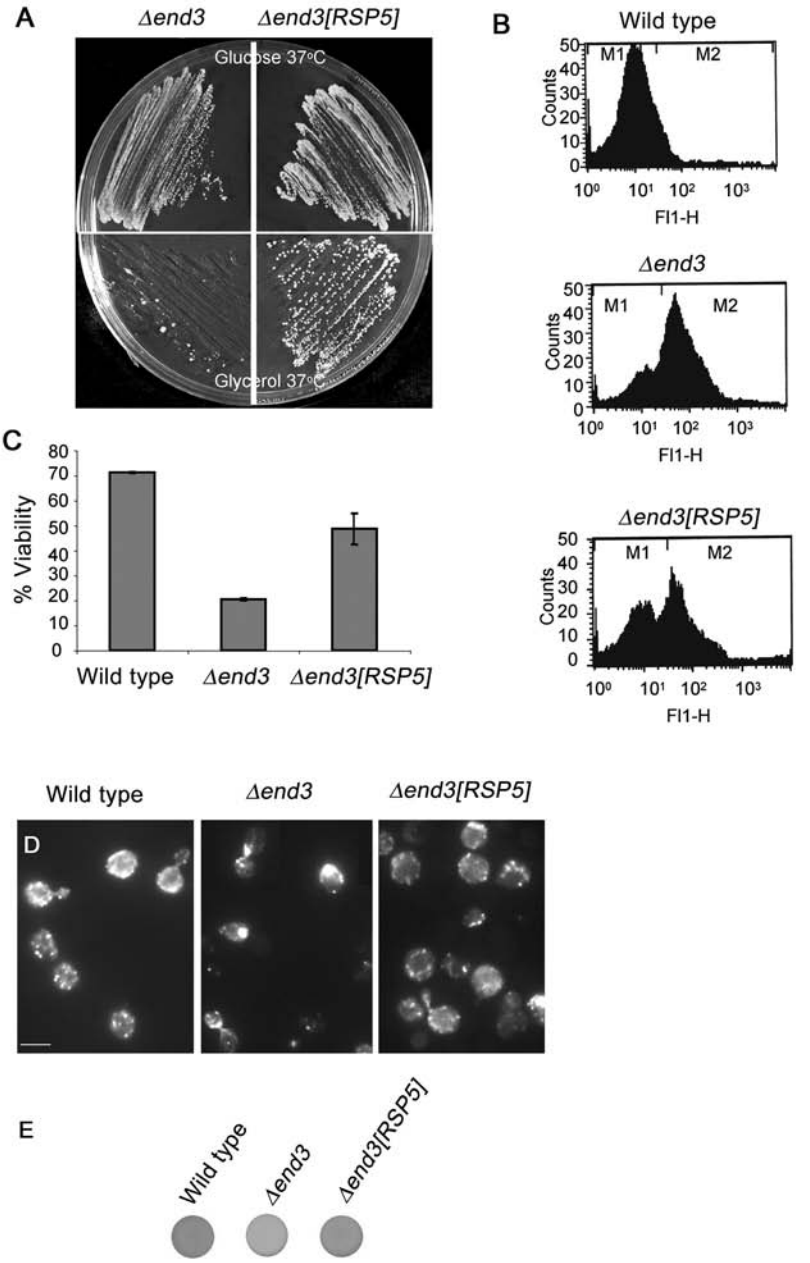

Fig. 6. Overexpression of *RSP5* can improve mitochondrial function, increase viability and restore actin dynamics in *Δend3* cells. (A) Wild-type, *Δend3* and *Δend3[RSP5]* cells were plated onto YP agar containing 2% glucose or 3% glycerol as the sole carbon source and grown for 3 days at 37°C. (B) Cultures from each of these strains were then assayed for ROS accumulation by flow cytometry using H_2DCFDA. (C) Cell viability was assessed via a plating assay carried out in triplicate. (D) Wild-type, *Δend3* and *Δend3[RSP5]* cells were grown to stationary phase and stained for F-actin with rhodamine-phalloidin. (E) The same strains were assayed for glycogen accumulation by iodine staining. Bar, 10 μm.

CAP/Srv2p is mislocalized in *Δend3* stationary-phase cells

How cells transduce signals to the reorganization of the F-actin cytoskeleton is a topic of great interest. A good candidate to link the Ras/cAMP signalling pathway to reorganization of the actin cytoskeleton is CAP/Srv2p (for a review, see Hubberstey and Mottillo, 2002). CAP/Srv2p can bind actin monomers and associates with the F-actin cytoskeleton (Lila and Drubin, 1997; Balcer et al., 2003). It acts to promote actin turnover by catalysing the release of ADP-actin monomers from filaments for nucleotide exchange (Balcer et al., 2003). CAP/Srv2p also

Journal of Cell Science

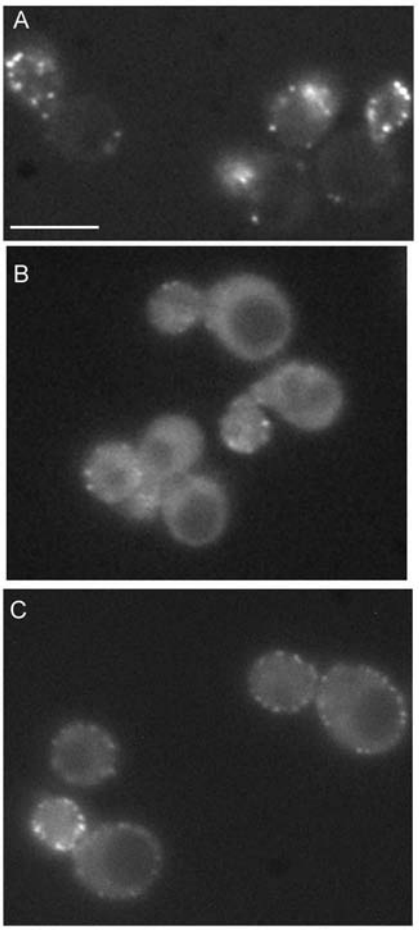

Fig. 7. Sla1p localization to the cortex in *Δend3* cells is enhanced by *RSP5* overexpression. (A) Wild-type, *Δend3* and *Δend3[RSP5]* cells expressing an integrated Sla1p-GFP were examined by fluorescence microscopy. In wild-type cells, Sla1p-GFP appeared as punctate spots that appear largely within the buds of dividing cells. (B) In *Δend3* cells, Sla1p appeared largely diffuse and cytoplasmic, and in a few punctate cortical structures. (C) In *Δend3[RSP5]* cells, the cytoplasmic staining was reduced and an increase in punctate cortical staining was observed in both mother and bud. Bar, 10 μm.

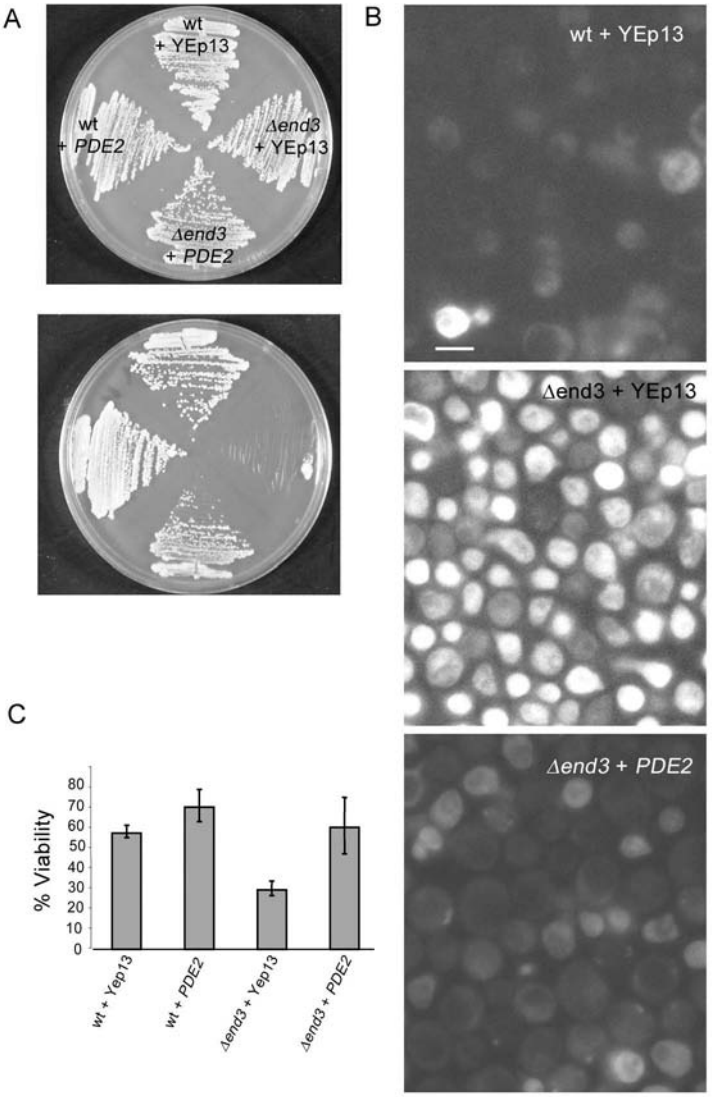

Fig. 8. *PDE2* overexpression reduces ROS accumulation in *Δend3* cells and restores viability. (A) Wild-type and Δend3 cells carrying either an empty Yep13 plasmid or Yep13 containing *PDE2* (Yep13[*PDE2*]) were struck onto YPD plates containing 0 mM or 3 mM H_2O_2 and grown for 3 days at 30°C. (B) ROS accumulation was assessed in wild-type cultures containing YEp13, *Δend3* cultures containing YEp13 and *Δend3* cultures containing Yep13[*PDE2*] that had been grown overnight in YPD at 30°C. Cells were visualized after staining by ultraviolet fluorescence microscopy. (C) The proportion of viable cells was assessed in overnight wild-type cultures containing YEp13, wild-type cultures containing YEp13[*PDE2*], *Δend3* cultures containing YEp13 and *Δend3* cultures containing YEp13[*PDE2*] cultures. Bar, 10 μm.

possesses an N-terminal adenylate-cyclase-binding site, which is important in transducing the Ras/cAMP signal (Yu et al., 1999). We were interested to establish whether the formation of F-actin aggregates in mutant cells had an effect on the localization of CAP/Srv2p, a scenario that might have a regulatory impact on Ras/cAMP signalling. CAP/Srv2p and F-actin were therefore visualized in wild-type and *Δend*3 cells during log and stationary phase (Fig. 10). As has previously been reported CAP/Srv2p partially colocalized with cortical F-actin patches in the budding cell of wild-type cells during log phase (Fig. 10A). A similar partial colocalization was observed in *Δend3* cells although, as described earlier, the cortical F-actin patches observed were larger and fewer (Fig. 10B). By contrast, F-actin patches observed in stationary-phase wild-type cells showed little colocalization with CAP/Srv2p, which appeared in very few punctate structures and was largely diffuse within the cell (Fig. 10C). Strikingly, CAP/Srv2p completely colocalised with the F-actin aggregates formed in *Δend3* stationary-phase cells and little diffuse staining was observed (Fig. 10D). This demonstrates that a dynamic actin cytoskeleton is required to regulate CAP/Srv2p localization during stationary-phase growth. The dramatic relocation of CAP/Srv2p from mainly diffuse cytoplasmic in wild-type cells to actin aggregates in *Δend3* stationary-phase cells might have functional consequences and so affect the role of CAP/Srv2p as an effector of Ras/cAMP signalling.

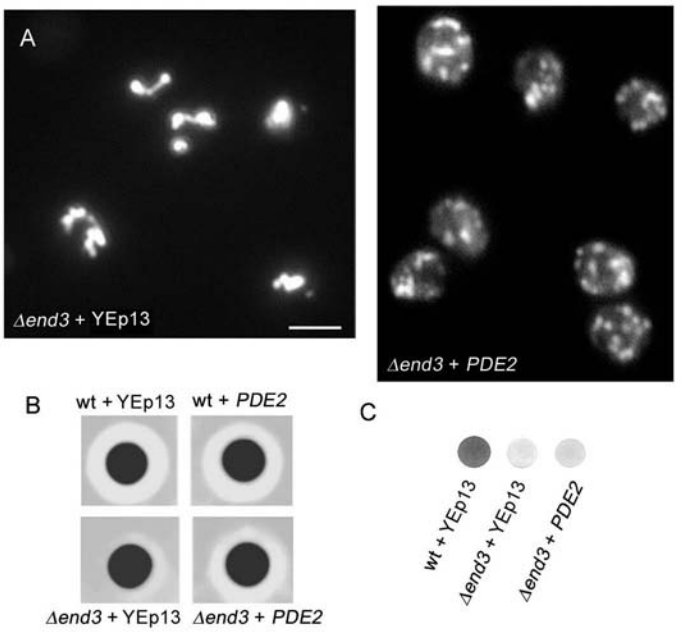

Fig. 9. Reduced actin dynamics of *Δend3* cells are increased by *PDE2* overexpression. (A) F-Actin was examined in overnight cultures of *Δend3* cells carrying either the YEp13 or YEp13 plasmid containing *PDE2*. (B) LatA-sensitivity halo assays were carried out on cells from wild-type cultures containing YEp13, wild-type cultures containing YEp13[*PDE2*], *Δend3* cultures containing YEp13 and *Δend3* cultures containing YEp13[*PDE2*]. (C) Glycogen accumulation was assessed in cells from wild-type cultures containing YEp13, *Δend3* cultures containing YEp13 and *Δend3* cultures containing YEp13[*PDE2*] cultures. (D) Heat-shock sensitivity was assessed in wild-type cultures containing YEp13, wild-type cultures containing YEp13[*PDE2*], *Δend3* cultures containing YEp13 and *Δend3* cultures containing YEp13[*PDE2*] cells. Bar, 10 μm.

Discussion

There is substantial evidence that the processes of ageing and apoptosis occur in yeast (for reviews, see Frölich and Madeo, 2001; Madeo et al., 2002b). It is proposed that apoptosis in unicellular organisms allows the selection of younger, fitter cells in times of environmental stress and so enhances the prospects of colony survival (Frölich and Madeo, 2000; Herker et al., 2004). It is therefore important to elucidate pathways that link environmental stress responses to apoptosis. We have previously demonstrated that altered F-actin dynamics correlate with ROS accumulation, cell longevity and apoptosis (Gourlay et al., 2004). Because actin remodelling forms an important part of the stress response, it is plausible that cytoskeleton dynamics play a central role in apoptosis signalling in response to these stresses.

A key factor in this proposed role for actin in apoptosis signalling is its close association with the mitochondrial network. Functional links between the two systems have been noted both in yeast (Boldogh et al., 1998; Simon et al., 1997; Simon et al., 1995) and in cells of higher eukaryotes (Morris and Hollenbeck, 1995). However, the studies in yeast have mostly focused on the role of actin in facilitating mitochondrial movement and inheritance. We have discovered that certain proteins that regulate the dynamics of the actin cytoskeleton during remodelling at the cell cortex are also important factors in the release of ROS from mitochondria. The stabilization of actin in *sla1Δ118-511*, *Δend3* or *end3-1* cells correlates with a decrease in mitochondrial membrane potential, an increase in oxidative stress and the development of apoptotic markers. We also demonstrated that the oxidative-stress burden originates from these mitochondria, because mutant strains that exhibit stabilized F-actin but lack mitochondrial DNA (*rho*^{0}) do not accumulate ROS. Furthermore, the addition of sublethal amounts of H_2O_2 to *Δend3* and *sla1Δ118-511* cultures resulted in a dose-dependent increase in detection of the early apoptotic marker PS. This suggests that *Δend3* and *sla1Δ118-511* cells exist close to an apoptotic threshold and implicates the cortical remodelling of actin as a mechanism that directly influences cell death in yeast.

An important question raised by this work is whether all mutations that reduce actin dynamics or perturb the cytoskeleton lead to mitochondrial dysfunction and ROS accumulation. We have analysed the ability of several strains deleted for cortical actin-regulatory proteins to grow using a glycerol carbon source and only those used in our detailed studies have a defect in this function. In addition, a mutation in the cofilin gene (*cof1-22*) that decreases actin dynamics by reducing the depolymerization rate of F-actin (Lappalainen and Drubin, 1997) does not have a defect in its ability to grow on glycerol, does not accumulate ROS and contains mitochondria with normal morphology and membrane potential (data not shown). These additional observations add to the idea that only a subset of actin-regulatory proteins are involved in the pathway that links actin dynamics to the functioning of the mitochondria and the release of ROS. This also argues that the effect investigated in this study are not due simply to a general reduction in actin dynamics from pleiotropic activities.

The deletion of *SLA1* or *END3* results in a similar actin-clumping phenotype and elicits the same effect of inducing oxidative stress. This implies that these proteins influence actin dynamics by a similar mechanism. Sla1p is thought to be involved in inhibiting activation of the Arp2/3 complex and so increasing depolymerization of actin at sites where remodelling is required (Rodal et al., 2003). One of the main reported roles of End3p is as a protein required for cortical recruitment of Sla1p (Warren et al., 2002). The targeting of Sla1p by End3p to sites of actin remodelling explains the similarity in phenotypes observed when the function of either protein is lost. The loss of both Sla1p or End3p function results in defects in endocytosis (Ayscough et al., 1999; Benedetti et al., 1994), although the effect of the *Δend3* mutation is more severe. This suggests that End3p has roles additional to the recruitment of Sla1p.

Another form of regulation that affects the function of Sla1p is ubiquitination. Although Sla1p has not been shown to be ubiquitinated directly, it has recently been reported that the ubiquitin ligase Rsp5p can bind directly to Sla1p (Stamenova et al., 2004). We show that overexpression of *RSP5* can rescue

Journal of Cell Science

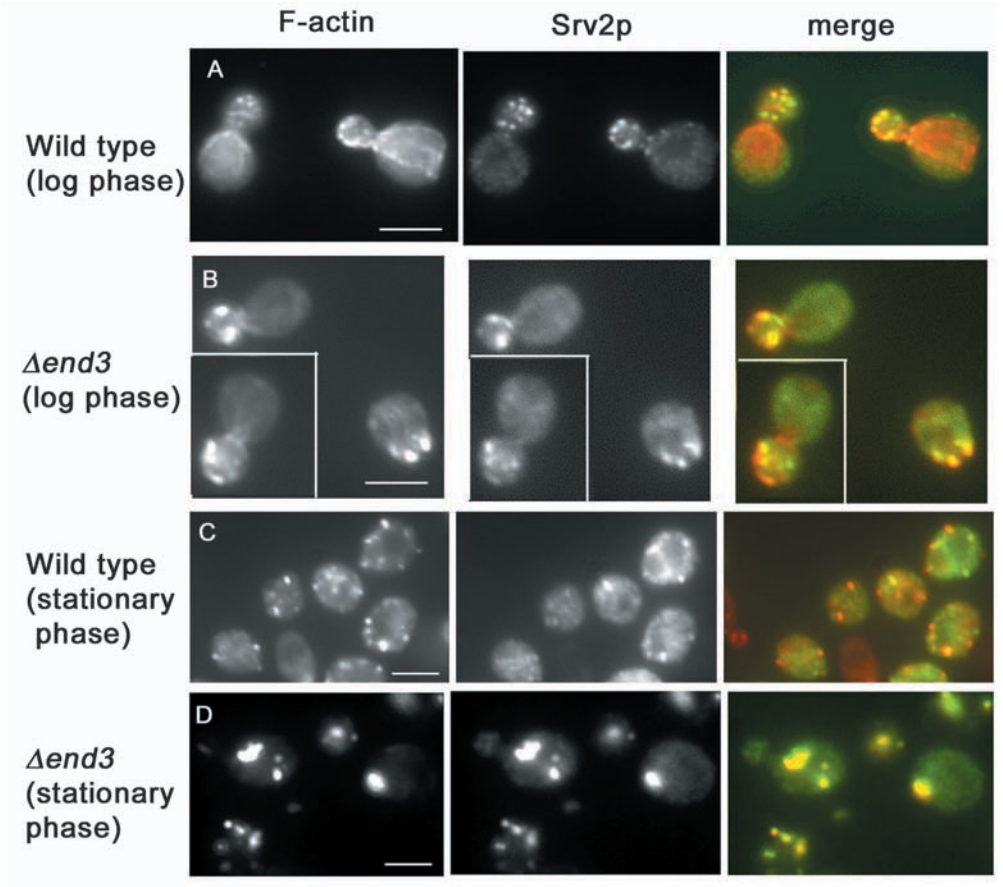

Fig. 10. CAP/Srv2p colocalization with F-actin in log- and stationary-phase wild-type and *Δend3* cells. F-Actin (red) and CAP/Srv2p (green) were visualized by fluorescence microscopy in wild-type (A,C) and *Δend3* (B,D) cells that had been grown to mid-log or stationary phase in liquid culture. Images were merged to observe areas of colocalization (yellow). Bars, 10 μm.

many of the defects associated with the loss of End3p. Indeed, *RSP5* overexpression rescues the ability of *end3*-null cells to grow on glycerol, reduces oxidative stress, increases viability and enhances the organization of the actin cytoskeleton. The loss of End3p targeting results in a reduction of Sla1p localization to cortical patches, which then accumulates in the cytosol. The overexpression of *RSP5* results in a marked increase in the amount of Sla1p localized to cortical patches. Our data suggest that the increased level of ubiquitination at the cell cortex acts to facilitate the formation of new binding sites for Sla1p, thereby bypassing the role for End3p in Sla1p recruitment. The relocalization of Sla1p then allows it to function relatively normally and to rescue the actin, mitchondrial and oxidative-stress phenotypes with which its mutation is associated.

The mechanism by which actin dynamics gives rise to ROS accumulation is unclear. One possibility is that F-actin filaments are involved in the regulation of the mitochondrial voltage-dependent anion channel (VDAC). It has been demonstrated in mammalian systems that the actin-regulatory protein gelsolin can protect against apoptosis by closing VDAC pores (Kusano et al., 2000). It has also been shown that in neuronal cells the antiapoptotic activity of gelsolin is actin dependent (Harms et al., 2004). In vitro studies have also demonstrated that actin can influence VDAC closure in *Neurospora crassa* (Xu et al., 2001). However, in our studies, the overexpression of the antiapoptotic proteins Bcl-2 or Bcl-xL, which are known to regulate VDAC closure, in *Δend3* cells have no effect on H_2O_2 sensitivity or culture viability (C.W.G. and K.R.A., unpublished). This suggests that ROS accumulation in *Δend3* cells occurs by a VDAC-independent mechanism.

Another alternative is that ROS build up occurs as a consequence of dysfunctional regulation of a stress-response pathway. In yeast, the Ras/cAMP pathway plays an important role in the control of growth and metabolism in response to nutritional status. In the presence of high glucose levels, Ras1/2p and CAP/Srv2p activate adenylate cyclase (Cyr1p) to catalyse cAMP production (for a review, see Rolland et al., 2002). The production of cAMP leads to PKA activation, which signals to the nucleus to inhibit a stress response and ensure G1 cell-cycle progression. Pde2p acts as a negative regulator of this pathway by hydrolysing cAMP, preventing PKA activation and derepressing the stress response. Our identification of Pde2p as a suppressor of actin aggregation and oxidative stress lends support to the idea that actin-cytoskeleton regulation is involved in the Ras/cAMP signalling cascade. In support of this link, it has been demonstrated that Ras2p is required for the regulation of actin in response to mild heat stress (Ho and Bretscher, 2001). The observation that CAP/Srv2p significantly colocalizes with cortical F-actin patches during log-phase but not stationary-phase growth might reflect an important regulatory event. Sequestration of CAP/Srv2p with F-actin aggregates in *Δend3* stationary-phase cells might in turn lead to perturbation of Ras/cAMP signalling and to some of the phenotypes observed in these cells. Interestingly, cells carrying the constitutively active $ras2^{val19}$ mutation display several phenotypic

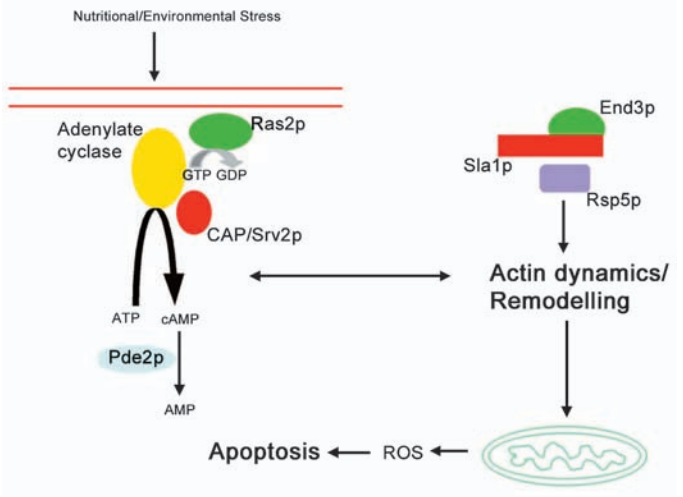

Fig. 11. Model linking Ras/cAMP signalling to actin remodelling, ROS release and apoptosis. In response to environmental stresses such as nutrient depletion or heat shock, the actin cytoskeleton undergoes remodelling as part of the survival response. Evidence suggests that the Ras/cAMP pathway is important in this remodelling. Also important are the actin-regulatory activities of Sla1p, which is targeted to the cortex by both End3p and Rsp5p activities. Inappropriate activation of the Ras/cAMP pathway or reduced actin dynamics as a result of a loss of Sla1p function lead to high levels of ROS accumulation. The exposure to high levels of oxidative stress lead to a reduced lifespan and an increased likelihood of apoptosis. We suggest that there is a cross-talk mechanism between the actin cytoskeleton and Ras/cAMP signalling machinery that regulates this pathway. This model provides a mechanism by which a colony of unicellular organisms can filter out older or genetically unfit individuals in response to environmental change.

similarities to *Δend3* and *sla1Δ118-511* cells. These include a failure to accumulate glycogen, a lack of adaptation to heat or nutritional stress (Sass et al., 1986; Care et al., 2004) (this study) and high levels of oxidative stress (Hlavata et al., 2003) (this study). This might indicate that *Δend3* and *sla1Δ118-511* exhibit elevated Ras/cAMP pathway activity. In support of this, the overexpression of the Ras/cAMP negative regulator Pde2p was able to rescue ROS accumulation and viability in *Δend3* and *sla1Δ118-511* cells. However, because *PDE2* overexpression in *Δend3* cells was unable to rescue glycogen-accumulation and heat-tolerance defects, this suggests that ROS accumulation occurs via a PKA-independent mechanism. Interestingly, Hlavata and colleagues also proposed (Hlavata et al., 2003) that $ras2^{val19}$ cells function via a PKA-independent pathway to generate ROS. We propose that there is a PKA-independent pathway in which F-actin remodelling is responsive to cAMP levels, with cytoskeletal aggregation acting as a trigger for ROS generation (Fig. 11). Further to this, we suggest that actin dynamics can act as biosensor of cellular health, linking environmental signalling via the Ras/cAMP pathway to apoptosis. In aged or genetically compromised cells, reduced actin dynamics would affect the ability of some cells to respond to environmental stress and to initiate an apoptotic response, which would eliminate them from the population and would promote the survival of the colony.

Thanks to F. Gardiner and P. Sudbery for critical reading of this manuscript, D. Drubin (University of California at Berkley) and H. Riezman (University of Basel, Switzerland) for yeast strains, T. Zoladek (Polish Academy of Sciences, Warsaw, Poland) for *RPS5* overexpression plasmids, and B. Westermann (Ludwig Maximilians University, Munich, Germany) for the mitochondrial GFP plasmid. This work was supported by a Medical Research Council (MRC) senior research fellowship to KRA (G117/394).

References

Ayscough, K. R. and Drubin, D. G. (1998). Immunofluorescence microscopy of yeast cells. In *Cell Biology: A Laboratory Handbook*, Vol. 2 (ed. J. Celis), pp. 477-485. New York: Academic Press.

Ayscough, K. R., Stryker, J., Pokala, N., Sanders, M., Crews, P. and Drubin, D. G. (1997). High rates of actin filament turnover in budding yeast and roles for actin in establishment and maintenance of cell polarity revealed using the actin inhibitor latrunculin-A. *J. Cell Biol.* **137**, 399-416.

Ayscough, K. R., Eby, J. J., Lila, T., Dewar, H., Kozminski, K. G. and Drubin, D. G. (1999). Sla1p is a functionally modular component of the yeast cortical actin cytoskeleton required for correct Localization of both Rho1p-GTPase and Sla2p, a protein with talin homology. *Mol. Biol. Cell* **10**, 1061-1075.

Balcer, H. I., Goodman, A. L., Rodal, A. A., Smith, E., Kugler, J., Heuser, J. E. and Goode, B. L. (2003). Coordinated regulation of actin filament turnover by a high-molecular-weight Srv2/CAP complex, cofilin, profilin, and Aip1. *Curr. Biol.* **13**, 2159-2169.

Benedetti, H., Raths, S., Crausaz, F. and Riezmann, H. (1994). The *END3* gene encodes a protein that is required for the internalization step of endocytosis and for actin cytoskeleton organization in yeast. *Mol. Biol. Cell* **1**, 1023-1037.

Boldogh, I., Vojtov, N., Karmon, S. and Pon, L. A. (1998). Interaction between mitochondria and the actin cytoskeleton in budding yeast requires two integral mitochondrial outer membrane proteins, Mmm1p and Mdm10p. *J. Cell Biol.* **141**, 1371-1381.

Boldogh, I. R., Yang, H. C., Nowakowski, W. D., Karmon, S. L., Hays, L. G., Yates, J. R., III and Pon, L. A. (2001). Arp2/3 complex and actin dynamics are required for actin-based mitochondrial motility in yeast. *Proc. Natl. Acad. Sci. USA* **98**, 3162-3167.

Can, J. and Reed, J. C. (2002). Yeast and apoptosis. *Nat. Rev. Mol. Cell. Biol.* **3**, 453-459.

Care, A., Vousden, K. A., Binley, K. M., Radcliffe, P., Trevethick, J., Mannazzu, I. and Sudbery, P. E. (2004). A synthetic lethal screen identifies a role for the cortical actin patch/endocytosis complex in the response to nutrient deprivation in *Saccharomyces cerevisiae*. *Genetics* **166**, 707-719.

Del Carratore, R., Della Croce, C., Simili, M., Taccini, E., Scavuzzo, M. and Sbrana, S. U. (2002). Cell cycle and morphological alterations as indicative of apoptosis promoted by UV irradiation in *S. cerevisiae*. *Mut. Res.* **513**, 183-191.

Droge, W. (2002). Free radicals in the physiological control of cell function. *Physiol. Rev.* **82**, 47-95.

Drubin, D. G., Miller, K. G. and Botstein, D. (1988). Yeast actin binding proteins: evidence for a role in morphogenesis. *J. Cell Biol.* **1107**, 2551-2561.

Finkel, T. U. R. (2003). Oxidant signals and oxidative stress. *Curr. Opin. Cell Biol.* **15**, 247-254.

Fröhlich, K. U. and Madeo, F. (2000). Apoptosis in yeast – a monocellular organism exhibits altruistic behaviour. *FEBS Lett.* **473**, 6-9.

Fröhlich, K. U. and Madeo, F. (2001). Apoptosis in yeast: a new model of ageing research. *Exp. Gerontol.* **37**, 27-31.

Gourlay, C. W., Carpp, L. N., Timpson, P., Winder, S. J. and Ayscough, K. R. (2004). A role for the actin cytoskeleton in cell death and aging in yeast. *J. Cell Biol.* **164**, 803-809.

Guthrie, G. and Fink, G. R. (1991). Generation of *rho*^{o} yeast strains. *Meths. Enzymol.* **194**, 150-151.

Hagan, I. M. and Ayscough, K. R. (2000). Fluorescence microscopy in yeast. In *Protein Localization by Fluorescence Microscopy: A Practical Approach* (ed. V. J Allan), pp. 179-205. Oxford, UK: Oxford University Press.

Harms, C., Bosel, J., Lautenschlager, M., Harms, U., Braun, J. S., Hortnagl, H., Dirnagl, U., Kwiatkowski, D. J., Fink, K. and Endres, M. (2004). Neuronal gelsolin prevents apoptosis by enhancing actin depolymerization. *Mol. Cell. Neurosci.* **25**, 69-82.

Herker, E., Jungwirth, H., Lehmann, K. A., Maldener, C., Fröhlich, K., Wissing, S., Büttner, S., Fehr, M., Sigrist, S. and Madeo, F. (2004). Chronological aging leads to apoptosis in yeast. *J. Cell Biol.* **164**, 501-507.

Hlavata, L., Aguilaniu, H., Pichova, A. and Nystrom, T. (2003). The oncogenic *ras2*^{val19} mutation locks respiration, independently of PKA, in a mode prone to generate ROS. *EMBO J.* **22**, 3337-3345.

Ho, J. and Bretscher, A. (2001). Ras regulates the polarity of the yeast actin cytoskeleton through the stress response pathway. *Mol. Biol. Cell* **12**, 1541-1555.

Holtzman, D. A., Yang, S. and Drubin, D. G. (1993). Synthetic-lethal interactions identify two novel genes, *SLA1* and *SLA2*, that control membrane cytoskeleton assembly in *Saccharomyces cerevisiae*. *J. Cell. Biol.* **122**, 635-644.

Honda, Y. and Honda, S. (1999). The *daf-2* gene network for longevity regulates oxidative stress resistance and Mn-superoxide dismutase gene expression in *Caenorhabditis elegans*. *FASEB J.* **13**, 1385-1393.

Hubberstey, A. V. and Mottilo, E. P. (2002). Cyclase-associated proteins: CAPacity for linking signal transduction and actin polymerisation. *FASEB J.* **16**, 487-499.

Jazwinski, S. M. (2002). Growing old: metabolic control and yeast aging. *Ann. Rev. Microbiol.* **56**, 769-792.

Kaminska, J., Gajewska, B., Hopper, A. K. and Zoladek, T. (2002). Rsp5p, a new link between the actin cytoskeleton and endocytosis in the yeast *Saccharomyces cerevisiae*. *Mol. Cell. Biol*. **22**, 6946-6948.

Karpova, T. S., Tatehill, K. and Cooper, J. A. (1995). Actin filaments in yeast are unstable in the absence of capping protein or fimbrin. *J. Cell Biol.* **131**, 1483-1493.

Koya, R. C., Fujita, H., Shimizu, S., Ohtsu, M., Takimoto, M., Tsujimoto, Y. and Kuzumaki, N. (2000). Gelsolin inhibits apoptosis by blocking mitochondrial membrane potential loss and cytochrome *c* release. *J. Biol. Chem.* **275**, 15343-15349.

Kusano, H., Shimizu, S., Koya, R. C., Fujita, H., Kamada, S., Kuzumaki, N. and Tsujimoto, Y. (2000). Human gelsolin prevents apoptosis by inhibiting apoptotic mitochondrial changes via closing VDAC. *Oncogene* **19**, 4807-4814.

Lappalainen, P. and Drubin, D. G. (1997). Cofilin promotes rapid actin filament turnover in vivo. *Nature* **388**, 78-82.

Laun, P., Pichova, A., Madeo, F., Fuchs, J., Ellinger, A., Kohlwein, S., Dawes, I., Fröhlich, K. U. and Breitenbach, M. (2001). Aged mother cells of *Saccharomyces cerevisiae* show markers of oxidative stress and apoptosis. *Mol. Microbiol.* **5**, 1166-1173.

Ligr, M., Madeo, F., Fröhlich, E., Hilt, W., Fröhlich, K. U. and Wolf, D. H. (1998). Mammalian Bax triggers apoptotic changes in yeast. *FEBS Lett.* **438**, 61-65.

Lila, T. and Drubin, D. G. (1997). Evidence for physical and functional interactions among two *Saccharomyces cerevisiae* SH3 domain proteins, an adenylyl cyclase-associated protein and the actin cytoskeleton. *Mol. Biol. Cell* **8**, 367-385.

Lin, Y. J., Seroude, L. and Benzer, S. (1998). Extended life-span and stress resistance in the *Drosophila* mutant *methuselah*. *Science* **282**, 943-946.

Longo, V. D., Gralla, E. B., and Valentine, J. S. (1996). Superoxide dismutase activity is essential for stationary phase survival in *Saccharomyces cerevisiae. J. Biol. Chem.* **271**, 12275-12280.

Ludovico, P., Sousa, M. J., Silva, M. T., Leao, C. and Corte-Real, M. (2001). *Saccharomyces cerevisiae* commits to a programmed cell death process in response to acetic acid. *Microbiology* **147**, 2409-2415.

Madeo, F., Fröhlich, E. and Fröhlich, K. U. (1997). A yeast mutant showing diagnostic markers of early and late apoptosis. *J. Cell Biol*. **139**, 729-734.

Madeo, F., Fröhlich, E., Ligr, M., Grey, M., Sigrist, S. J., Wolf, D. H. and Fröhlich, K. U. (1999). Oxygen stress: a regulator of apoptosis in yeast. *J. Cell Biol.* **145**, 757-767.

Madeo, F., Herker, E., Maldener, C., Wissing, S., Lachelt, S., Herlan, M., Fehr, M., Lauber, K., Sigrist, S. J., Wesselborg, S. et al. (2002a). A caspase-related protease regulates apoptosis in yeast. *Mol Cell.* **9**, 911-917.

Madeo, F., Engelhardt, S., Herker, E., Lehmann, N., Maldener, C., Proksch, A., Wissing, S. and Fröhlich, K. U. (2002b). Apoptosis in yeast: a new model system with applications in cell biology and medicine. *Curr. Genet.* **41**, 208-216.

Martindale, J. and Holbrook, N. (2002). Cellular response to oxidative stress: signaling for suicide and survival. *J. Cell Physiol.* **192**, 1-15.

Migliaccio, E., Giorgio, M., Mele, S., Pelicci, G., Reboldi, P., Pandolfi, P. P., Lanfranconne, L. and Pelicci, P. G. (1999). The p66^{shc} adaptor protein controls oxidative stress response and life span in mammals. *Nature* **402**, 309-313.

Morris, R. L. and Hollenbeck, P. J. (1995). Axonal transport of mitochondria along microtubules and F-actin in living vertebrate neurons**.** *J. Cell Biol.* **131**, 1315-1326.

Nestelbacher, R., Laun, P., Vondrakova, D., Pichova, A., Schuller, C. and Breitenbach, M. U. (2000). The influence of oxygen toxicity on yeast mother cell-specific aging. *Exp. Gerontol.* **35**, 63-70.

Ohtsu, M., Sakai, N., Fujita, H., Kashiwagi, M., Gasa, S., Shimizu, S., Eguchi, Y., Tsujimoto, Y., Sakiyama, Y., Kobayashi, K. et al. (1997). Inhibition of apoptosis by the actin-regulatory protein gelsolin. *EMBO J.* **16**, 4650-4656.

Rodal, A. A., Manning, A. L., Goode, B. L. and Drubin, D. G. (2003). Negative regulation of yeast WASp by two SH3 domain-containing proteins. *Curr. Biol.* **13**, 1000-1008.

Rolland, R., Winderickx, J. and Thevelin, J. M. (2002). Glucose sensing and signaling mechanisms in yeast. *FEMS Yeast Res.* **2**, 183-201.

Sass, P., Field, J., Nikawa, J., Toda, T. and Wigler, M. (1986). Cloning and characterisation of the high-affinity cAMP phosphodiesterase of *Saccharomyces cerevisiae. Proc. Natl. Acad. Sci. USA* **83**, 9303-9307.

Simon, V., Swayne, T. and Pon, L. (1995). Actin-dependent mitochondrial motility in mitotic yeast and cell-free systems: identification of a motor activity on the mitochondrial surface. *J. Cell Biol.* **130**, 345-354.

Simon, V. R., Karmon, S. L. and Pon, L. A. (1997). Mitochondrial inheritance: cell cycle and actin dependence of polarised mitochondrial movements in *Saccharomyces cerevisiae*. *Cell Motil. Cytoskeleton* **37**, 199-210.

Stamenova, S. D., Dunn, R., Adler, A. S. and Hicke, L. (2004). The Rsp5 ubiquitin ligase binds to and ubiquitinates members of the yeast CIN85-endophilin complex, Sla1-Rvs167. *J. Biol. Chem.* **279**, 16017-16025.

Tissenbaum, H. and Guarente, L. (2002). Model organisms as a guide to mammalian ageing. *Dev. Cell* **1**, 9-19.

Warren, D. T., Andrews, P. D., Gourlay, C. W. and Ayscough, K. R. (2002). Sla1p couples the yeast endocytic machinery to proteins regulating actin dynamics. *J. Cell Sci.* **115**, 1703-1715.

Wawryn, J., Krzepilko, A., Myszka, A. and Bilinski, T. (1999). Deficiency in superoxide dismutases shortens life span of yeast cells. *Acta Biochim. Pol.* **46**, 249-253.

Westermann, B. and Neupert, W. (2000). Mitochondria-targeted green fluorescent proteins: convenient tools for the study of organelle biogenesis in *Saccharomyces cerevisiae*. *Yeast* **16**, 1421-1427.

Xu, X., Forbes, J. G. and Colombini, M. (2001). Actin modulates the gating of *Neurospora crassa* VDAC. *J. Membr. Biol.* **180**, 73-81.

Yu, J., Wang, C., Palmieri, S. J., Haarer, B. K. and Field, J. (1999). A cytoskeletal localizing domain in the cyclase-associated protein, CAP/Srv2p, regulates access to a distant SH3-binding site. *J. Biol. Chem.* **274**, 19985-19991.

Journal of Cell Science